Biogeosciences Discussions, 2, 37–75, 2005
www.biogeosciences.net/bgd/2/37/
SRef-ID: 1810-6285/bgd/2005-2-37
European Geosciences Union

Biogeosciences Discussions

Biogeosciences Discussions is the access reviewed discussion forum of *Biogeosciences*

Control of phytoplankton production by physical forcing in a strongly tidal, well-mixed estuary

X. Desmit[1], J. P. Vanderborght[1], P. Regnier[2], and R. Wollast[1, †]

[1]Laboratory of Chemical Oceanography and Water Geochemistry and Department of Water Pollution Control, Université Libre de Bruxelles, Boulevard du Triomphe (CP208), 1050 Brussels, Belgium
[2]Biogeochemical System Dynamics, Department of Geochemistry, Utrecht University, 3508 TA Utrecht, The Netherlands
† Deceased on 28 July 2004

Received: 29 December 2004 – Accepted: 7 January 2005 – Published: 14 January 2005

Correspondence to: X. Desmit (xdesmit@ulb.ac.be)

Abstract

A model for phytoplanktonic production in turbid, macro-tidal estuaries is proposed. It is based on the description of light-dependent algal growth, phytoplankton respiration and mortality. The model is forced by solar irradiance, mixing depth and light penetration. The extinction coefficient is directly related to the dynamics of suspended particulate matter. Model results show that the description of phytoplankton growth must operate at a time resolution sufficiently high to describe the interference between solarly and tidally driven physical forcing functions. It also demonstrates that in tidal and turbid estuaries, the short-term variation of the euphotic depth to mixing depth ratio has to be resolved for production estimates and that net positive phytoplankton production can be achieved in areas of high turbidity. The model is used to explain the typical phytoplankton decay observed along the longitudinal gradient of salinity in turbid estuaries, using the Western Scheldt as an example.

1 Introduction

Estuaries are often subject to high nutrient loads, which may lead to local eutrophication of the water masses. In turbid estuaries, however, phytoplankton respiration can exceed biomass production because of the low light penetration into the water column. This results in a negative depth-integrated net primary production (NPP) (Grobbelaar, 1985; Reid et al., 1990; Cole et al., 1992; Heip et al., 1995). Nevertheless, high phytoplankton biomass concentrations are commonly observed in these environments (Kromkamp et al., 1995; Kromkamp and Peene, 1995; Heip et al., 1995 and references therein). Various authors have used the "critical mixing depth" approach introduced by Sverdrup (1953) to explain this apparent contradiction (Cole et al., 1992; Fichez et al., 1992; Irigoien and Castel, 1997). It is indeed well established that net phytoplankton production is determined by the ratio between euphotic and mixing depths, which are mainly controlled by pure physical forcing mechanisms (Sverdrup, 1953; Grobbe-

laar, 1985; Cloern, 1987; Cole and Cloern, 1987; Falkowski and Raven, 1997). This control is particularly critical in turbid environments such as estuaries and coastal waters, which are often under the influence of significant particulate terrigeneous fluxes (Postma, 1980).

Phytoplankton production models currently incorporate an increasingly complex description of underlying biological mechanisms such as intracellular fluxes (Lancelot et al., 1986; Reid et al., 1990; Williams and Lefèvre, 1996), food-web interactions (Soetaert et al., 1994; Lancelot et al., 2000), photoacclimation (Cullen and Lewis, 1988; Geider et al., 1996; Geider et al., 1998). In contrast, as pointed out for instance by Fichez et al. (1992), most studies on estuarine phytoplankton production have neglected the problems of fluctuating light regime as a major controlling factor. In particular, the coupling between primary production and sediment dynamics has been overlooked in the past, partly because the study of these processes pertains to scientific disciplines that have largely evolved independently. Many authors have studied the correlation between phytoplankton prodution and turbidity, using the composite parameter BZE: biomass B, euphotic depth Z and solar irradiance E (Cole and Cloern, 1984; Harding et al., 1986; Cole and Cloern, 1987; Keller, 1988; Cole, 1989; Boyer et al., 1993; MacIntyre and Cullen, 1996). This empirical model may explain a large part of the variability of phytoplankton production in many estuaries, especially at the seasonal scale. However, the BZE model does not rely upon one physiological basis. In particular, it lacks any description of the phytoplankton response to light intensity (MacIntyre and Cullen, 1996). More critically, it does not link the value of the euphotic depth to the suspended particulate matter (SPM) dynamics.

In this paper, the focus is on nutrient-rich, well-mixed tidal estuaries, where phytoplankton growth is not limited by nutrient availability, but where light is the crucial control factor. In such systems, it is expected that the underwater light field is not only determined by the incident solar irradiance, but also by the tidal influence on hydrodynamics and sediment transport (Wofsy, 1983). Estimating the combined effect of these forcing processes on the spatio-temporal evolution of phytoplankton production is clearly

not a trivial question. The scope of this study is therefore to assess how short-term, tidally driven physical forcing mechanisms interfere with the incident sunlight energy to sustain phytoplankton production in these environments. The impact of chlorophyll *a* resuspension on the estimate of depth-integrated phytoplankton production is also discussed. The paper is structured as follows: first, a simple model of phytoplankton biomass for strongly tidal, well-mixed estuaries is presented. It is then applied to an idealized case using simple periodic forcing functions, in order to highlight the main features of the systems response. Finally, more complex forcing conditions are applied, taking the Scheldt estuary (B, NL) as an example of a typical well-mixed, turbid system displaying a high dynamical suspended matter behavior (Fettweis et al., 1998).

2 Model description

The main purpose of this study is to investigate whether or not a positive algal growth can be sustained in a turbid, well-mixed estuary, where the mixing depth is larger than the euphotic depth. To answer this question, we hypothesize that the turbidity, and hence the light regime, is essentially controlled by local hydrodynamic conditions. In other words, the dynamics of suspended particulate matter (SPM) results mainly from local exchange fluxes with the bed through the processes of resuspension and deposition. This implies that the instantaneous current velocity is the key factor for turbidity. In addition, our focus is on the effect of local physical conditions on the sustainability of local algal growth; it is not on the effect of advective or diffusive transport on phytoplankton concentration along the longitudinal gradient. As a result, a simple box approach is adequate for our purpose. The use of more complex transport-reaction models of the estuarine continuum (e.g. Regnier and Steefel, 1999; Vanderborght et al., 2002) is therefore not required.

2.1 Governing equations for a well-mixed reservoir of oscillating depth

Consider a well-mixed reservoir of unit surface area, whose volume is changing with time due to the tidal variation of the depth z_{max} (Fig. 1). The volume change is caused by a flow $Q(t)$ that is either positive or negative to account for level rise and level fall, respectively. To avoid dilution effects, the water added or withdrawn always has the same composition (including biomass and SPM concentration) as the water inside the reservoir. Solar light penetrating into the water is gradually attenuated within the water column: this well-mixed system is thus 0-D with respect to space for all constituents (including turbidity), yet it is a 1-D (vertical) system for photosynthetically active radiation (PAR). As a result, the governing equation must be written in terms of the total biomass B_{tot} within the reservoir:

$$\frac{dB_{tot}}{dt} = QB + \int_0^{z_{max}} r(z,t)\, dz, \tag{1}$$

where $r(z,t)$ is the rate of phytoplankton biomass production at any time t and depth z within the reservoir. The algal biomass B is related to B_{tot} according to:

$$B = \frac{B_{tot}}{z_{max}}, \tag{2}$$

while the rate of change of the water depth is given by:

$$\frac{dz_{max}}{dt} = Q(t). \tag{3}$$

2.2 Rate of algal growth

The rate r of phytoplankton biomass production is given by:

$$r = \text{NPP} - \text{Excr} - \text{Mor}, \tag{4}$$

where NPP is the net primary production of phytoplankton, Excr is the excretion rate (release of dissolved organic carbon) and Mor is the mortality rate of the algal cells. The net primary production is defined as:

$$\text{NPP} = \text{GPP} - \text{Resp}, \tag{5}$$

where GPP is the gross primary production of phytoplankton and Resp is the algal respiration rate. All rates are usually expressed in μgC.L^{-1}.h^{-1}.

The relationship between GPP and PAR (in μmol quanta.m^{-2}.s^{-1}) is modeled according to Platt's equation (Platt et al., 1980; MacIntyre et al., 2002):

$$\text{GPP} = B\, P^B_{max} \left(1 - e^{-\frac{\alpha^B PAR}{P^B_{max}}} \right), \tag{6}$$

where the algal biomass B is usually given in units of μg Chlorophyll a.L^{-1}. α^B is the specific photosynthetic efficiency and P^B_{max} is the specific light-saturation rate of photosynthesis. Values and units for these parameters are presented in Table 1.

At least two additional processes are known to influence phytoplankton productivity: photoacclimation and photoinhibition. Experimental evidences of short-time photoacclimation, inducing changes in the photosynthetic parameters, have been previously obtained at the diel scale in turbid systems (see e.g. Harding et al., 1986; Prézelin, 1992). However, some authors argued that in a well-mixed and turbid water column, where the light history of algal cells is highly depending on turbulent mixing (Cullen and Lewis, 1988), phytoplankton is acclimated to a mean irradiance between the bottom and the surface (Demers et al., 1986; Mallin and Paerl, 1992). More recently, a number of authors have tried to link this variation of the photosynthetic parameters with the internal molecular machinery of the chloroplast (Geider et al., 1997; Kana et al., 1997; MacIntyre et al., 2002; Han, 2002). However, it remains difficult to transcript those detailed physiological description in the context of environmental modelling, especially when hydrodynamics is not resolved vertically (as it is the case in this paper). Also, it is difficult to identify from the experimental data what part of photoacclimation

must be attributed to the incubation process, and what part may be attributed to the natural forcings in the environment. The consensus is thus not yet reached to know how far we must consider the short-time photoacclimation in the case of a turbid and tidal estuary. Though it is not the purpose of the present paper to answer this question, we have simulated different diel-variations of the photosynthetic parameters to see how such possible changes could affect our conclusions (see end of discussion).

When subjected to surface irradiances, phytoplankton cells may suffer photoinhibitory effects, especially when acclimated to low-light intensities (Mallin and Paerl, 1992; MacIntyre and Cullen, 1996). However, photoinhibition is not an instantaneous process (Melis, 1999), and the time-scale for full development of photoinhibition may vary between 0.5 and 1.5 h (Pahl-Wostl and Imboden, 1990). Thus, it is reasonable to assume that the response time of photoinhibition to changes in light regime is larger than the residence time of the cells near the water surface (Macedo et al., 1998). As a result, photoinhibition is ignored in Eq. (6). This hypothesis is obviously not valid in shallow estuaries, where light is available down to the bottom.

A proper parameterization of the phytoplankton respiration term is of crucial importance for our purpose. The simplest formulation for the respiration rate (Resp) is that it is simply a constant percentage of $P^B_{\max}$ (Steemann Nielsen and Hansen, 1959). Many authors have adopted this expression, using various coefficients of proportionality for different algal species (Gilstad et al., 1993; Langdon, 1993 and references therein). In light-limited environments where phytoplankton production is far from saturation, such an approach will lead to an overestimation of the respiration rate. Other formulations, which take into account intracellular mechanisms, have been proposed (Langdon, 1988; Lancelot et al., 1991; Lewitus and Kana, 1995; Lancelot et al., 2000) and are in agreement with laboratory measurements carried out on specific cultures of phytoplankton (Falkowski and Raven, 1997). In these models, algal respiration is divided into a maintenance term (R_m) associated to basal metabolism and a growth or biosynthesis term (R_g). This approach takes into account the light-dependency of respiration. For instance, some diatoms show a respiration rate in the light almost twice as

large as in the dark (Weger et al., 1989). Following Langdon (1993), R_g is expressed here as a fraction of GPP. R_m is simply proportional to the algal biomass:

$$\text{Resp} = R_m + R_g \tag{7}$$

with

$$R_m = \rho_m \; B\theta \tag{8}$$

and

$$R_g = \rho_g \; \text{GPP}, \tag{9}$$

where ρ_m is the rate constant for maintenance respiration, θ is the carbon:chlorophyll *a* ratio and ρ_g (comprised between 0 and 1) is the growth respiration factor.

To model the excretion rate of dissolved organic carbon (DOC), we follow the hypothesis that it is related to photosynthesis (Mague et al., 1980; Lancelot et al., 2000). Excr is thus expressed as:

$$\text{Excr} = \varepsilon \; \text{GPP}, \tag{10}$$

where ε is the excretion factor. There is no typical value for ε, though common values are reported to be comprised between 0.03 and 0.2 (Malinsky-Rushansky and Legrand, 1996; Hansell and Carlson, 1998; Morán and Estrada, 2002). We hypothesize that in a nutrient-rich and light-limited system, algae are expected to allocate the major part of recent photosynthate to the biosynthesis of cellular constituents, instead of excreting it as DOC (Otero and Vincenzini, 2004). For this reason, a small ε value (0.03) has been used in the model.

The mortality of phytoplankton is described by a first order equation (Fasham, 1995):

$$\text{Mor} = m\, B\theta, \tag{11}$$

where m is the mortality rate constant. In our conceptual model, the grazing of phytoplankton is not explicitly described and is therefore included in the overall mortality term.

In well-mixed turbid waters, where light-scattering and light-absorbing particles are uniformly distributed, an approximately exponential decrease of the scalar irradiance is observed over depth (Di Toro, 1978). The time and depth variations of PAR may thus be described according to:

$$\mathrm{PAR}(z,t)=E_0(t)e^{-k_d(t)z}, \tag{12}$$

where E_0 (t) is the surface PAR and k_d (t) is the vertical attenuation coefficient for scalar irradiance (Kirk, 1994). Since the system is vertically well mixed, k_d can be taken as constant within the water column. Combining Eqs. (4) to (12) allows the computation of the rate of phytoplankton biomass production r at any time t and depth z:

$$r(z,t) = B(z,t)\left[P^B_{\max}\left(1-e^{-\frac{\alpha^B E_0 e^{-k_d z}}{P^B_{\max}}}\right)\left(1-\rho_g-\varepsilon\right)-(k_m+m)\right]. \tag{13}$$

Substitution of $r(z,t)$ by expression (13) in Eq. (1) leads to an exponential-integral which has no exact solution in terms of elementary functions, and hence must be integrated numerically. As it appears from the equation above, the time dependence of $r(z,t)$ is ultimately controlled by the external forcing functions E_0 (t) and k_d (t). The variable $z_{\max}$ (t) which appears in Eq. (1) introduces a supplementary forcing function with respect to time due to the tide. Internal model parameters are α^B and $P^B_{\max}$.

3 Forcing conditions

As pointed out in the previous section, three forcing functions have to be specified to compute the temporal change of phytoplankton biomass: the incident PAR E_0 (t), the vertical light attenuation coefficient k_d (t) and the total depth $z_{\max}$ (t), which is also equal to the mixing depth, and is generally larger than the euphotic depth in strong tidal, turbid estuaries. In a first set of simulations, these parameters are expressed in terms

of simple periodic functions. The purpose of this simplified setting is to advance our conceptual understanding of the mechanistic interactions between the various physical forcing functions. The incident PAR E_0 has been estimated from a classical astronomical routine, taking also into account the atmospheric absorption of incident solar energy and the ratio of PAR to total irradiance. The grey line in Fig. 2 shows the temporal variation of E_0 that has been used for the simulations. It is typical for a cloudless, summer period (4 to 9 July) at latitude 52° N.

Following the hypothesis that the current velocity is the key control factor for SPM and turbidity, the resulting tidal variation of the light absorption coefficient k_d is approximated by a sine function of period 6 h 12 min. This value corresponds to half the period of the M2 tidal harmonic (black line, Fig. 2) and allows reproducing the occurrence of two turbidity minima per tidal cycle, corresponding to low- and high-water slacks. Conversely, two turbidity maxima are also simulated, for maximum ebb and flood velocities respectively. The values selected for k_d (between 2 and 16 m^{-1}) are typical of turbid estuaries (Cloern, 1987). The resulting variation of the euphotic depth (defined as the depth where PAR is equal to 1% of the surface value) is represented in Fig. 3. Finally, the mixing depth $z_{\max}$ is also modeled using a sine function, but this time with a period 12 h 25 min. A set of scenarios is considered, ranging from a relatively shallow reservoir (mean $z_{\max}$=6 m) to deeper systems (mean $z_{\max}$=20 m) with a tidal amplitude maintained to 6 m (Fig. 3). In all cases, the euphotic depth, which is comprised between 0.3 and 2.3 m, represents only a small fraction of the mixing depth.

In a second set of simulations, we introduce the influence of natural variability on the forcing functions E_0, k_d and $z_{\max}$, and we investigate the consequence of this variability on the primary production. Our purpose is to verify that the first-order features obtained in the previous set of simulations remain valid when more complex situations are described. By comparing the results of these simulations with experimental observations, we also aim at a validation of the model approach. The forcing functions are now parameterized from field data and from model results obtained for the Western Scheldt estuary (Belgium–The Netherlands), which can be considered as a typical example

of a macro-tidal, turbid environment (Wollast, 1988). Two situations are considered, which differ in k_d as well as in z_{max} (the incident PAR E_0 being identical in both cases). The first situation corresponds to a shallow site (location 1, representative of the fresh water zone situated in the tidal estuary, about 110 km of the estuarine mouth), while the second situation considers a deeper area of the estuary (location 2, typical of the brackish area around the harbour of Antwerp, 80 km from the estuarine mouth). For E_0 (t), the same astronomical routine as above is used, but the resulting incident solar radiation is modified using a measured cloud coverage factor for temperate regions (July 1999, data supplied by IRM (1999), Fig. 4). The light attenuation coefficient k_d (t) has been obtained from a large number of vertical light profiles and SPM measurements conducted throughout 2002. It is expressed as an explicit function of SPM:

$$k_d = 1.4 + 0.0592\ \mathrm{SPM} \tag{14}$$

with k_d in m^{-1} and SPM in $mg.L^{-1}$ (Fig. 5). The in situ determination of the scalar absorption coefficient k_d has been performed using two spherical quantum sensors (Aquamatic AQPL-UV912) separated by a constant, known vertical distance. This technique eliminates the need for incident light compensation and allows the continuous logging of the k_d value. An example of results for the Scheldt is given in Fig. 6. In addition, vertical profiles of scalar irradiance have repeatedly shown that the k_d value can be considered as constant with depth in this well-mixed estuary, at least in the euphotic layer (Fig. 7).

In the second set of simulation, the SPM concentration is estimated using the concept of maximum transport capacity, which allows expressing the particulate matter content as a function of the local instantaneous current velocity and water depth (Verbanck, 2003):

$$\mathrm{SPM} = X \frac{|u|^5}{z_{max}^2} + Y, \tag{15}$$

where $|u|$ is the modulus of the cross-sectional averaged velocity and X, Y two constants. The two variables u and z_{max} are obtained from a one-dimensional hydrody-

namic (HD) model of the Western Scheldt estuary (Regnier et al., 1998), which not only resolves the tidal timescale, but also incorporates the longer term neap-spring oscillation and the variation of the freshwater discharge. For the shallow zone (Fig. 8a), z_{max} is comprised between 4 and 9 m; in the deeper area (Fig. 8b), a z_{max} value varying between 10 and 16 m is used.

In Eq. (15) above, the constant term Y corresponds to the finer particulate material, which always stays in suspension in the water column (wash load). The coefficient Y is essentially dependent on the nature of the suspension, which can vary along the estuarine gradient. In order to reproduce the SPM concentration range commonly observed in the two areas, distinct values for the constants (X, Y) have been used for the simulation: $X=2\times10^3$ and $Y=40$ for the shallow, freshwater tidal estuary; $X=6\times10^3$ and $Y=25$ for the deeper, brackish region. The resulting variations of k_d for both situations is represented in Fig. 9. Despite its simplicity, this approach provides a realistic first-order description of the SPM and k_d dynamics, as shown by the comparison between the turbidity measured at a monitoring station located in a zone of high SPM content (km 80 from the mouth) and the results of a simulation carried out for the same location (Figs. 10b and 10c). Two peaks per tidal cycle can be observed, corresponding to maximum ebb and flow velocities. The very fast settling of suspended solids at slack water is another salient feature of the observed and modelled SPM dynamics.

Because the tidal velocities computed by the HD model are essentially similar in the shallow and deeper areas, the SPM, and hence the k_d, differ mainly via the influence of z_{max}, according to Eq. (15). Comparing Figs. 9a and 9b shows indeed that the resulting k_d is on average higher at the shallow site than at the deeper site. In both cases, the water depth and the light attenuation coefficient are strongly modulated by the spring-neap oscillations.

4 Dynamics of phytoplankton growth

4.1 First set of simulations

The results of the simulations obtained when using simple, periodic forcing functions for E_0, k_d and z_{max} are synthesized in Figs. 11 to 13. Figure 11 shows the time evolution of the PAR, 20 cm below the water surface. A complex temporal pattern is obtained, which results from the modulation of E_0(t) by k_d (t). Because these two signals have different frequencies, the underwater PAR shows two or three daily peaks with a progressive phase shift in the daily maximum. This idealized simulation demonstrates that the maximum underwater PAR is most of the time not synchronized with solar noon: synchronism with solar noon ($\pm^1/_2$ h) actually occurs every 6 to 7 days, as a result of the interaction between lunar (tide) and solar (night-day) forcing functions.

Similar dynamics are predicted for the depth-integrated gross phytoplankton production (GPPz). It is illustrated in Fig. 12 (black line), a result that is valid for the whole set of simulations because the water depth is always greater than the euphotic depth. However, the non-linear relationship between GPP and PAR (Eq. 6) tends to flatten the multiple productivity peaks within one day. The simulation leads to the rather unexpected result that, in some instances (e.g. day 185), the highest instantaneous depth-integrated GPP may occur at 09:00 a.m. and again at 03:00 p.m. (solar time), although the incident solar light is far from its maximum at these moments.

A very different response is predicted if an average k_d value is used for the simulation (Fig. 12, grey line). Obviously, the GPPz is then directly related to the time evolution of E_0 (t). More importantly, the depth- and time-integrated GPP is significantly different whether a time dependent or a constant mean k_d value is used. In the latter case, the integrated value over one month is lower by a factor of 30%. This is of course a consequence of the non-linear relationship between GPP and k_d.

One may argue that sedimentation and resuspension mechanisms, that control the SPM dynamics, could affect similarly phytoplankton cells. In some estuaries, short-term variations of chlorophyll *a* have been observed simultaneously with changes in

turbidity (Demers et al., 1987; de Jonge and van den Bergs, 1987; Cloern et al., 1989; Litaker et al., 1993; Lucas, 2003). MacIntyre and Cullen (1996) even conclude that the decrease in mean irradiance caused by resuspension is compensated for by a concomitant increase in suspended chlorophyll *a*, and hence has a negligible influence on GPPz estimates. However, chlorophyll *a* resuspension is only reported in shallow estuaries (<2.5 m) or in the shallower areas of deeper estuaries (such as tidal flats <60 cm), where benthic diatoms may often be found. In this paper, we examine systems where the mixing depth is predominantly greater than the euphotic depth, a condition that is not extremely favourable to the development of benthic microalgae (Muylaert et al., 2002). To verify this assumption, simultaneous measurements of turbidity and chlorophyll *a* have been performed at various depths in the Scheldt estuary (oligo- and mesohaline regions) during a number of tidal cycles. These measurements have never shown any strong, positive correlation between SPM and chlorophyll *a*, suggesting that, in this type of environment, short-term variations in phytoplankton concentration are essentially due to the advection of water masses, rather than to phytoplankton settling and resuspension.

The effect of z_{max} on the net phytoplankton growth is illustrated in Fig. 13 for the whole set of scenarios. As z_{max} increases, the processes responsible for phytoplankton decay (maintenance respiration and mortality) become gradually predominant in the value of r (Eq. 13). As a result, the phytoplankton biomass shows an increasing pattern in the shallow reservoirs scenarios, while it approaches a typical exponential decrease in the deep reservoirs scenarios. For the same reason, daily oscillations are noticeable when the euphotic to mixing depth ratio is high. They tend to be progressively damped out when this ratio decreases.

4.2 Second set of simulations

The application of simplified periodic forcing functions to the case of a well-mixed, oscillating-depth reservoir gives a conceptual understanding of the coupling between sediment dynamics, light climate in the water column and phytoplankton production. To

advance one step further in the analysis, more complex forcing functions are now considered. They are typical of two locations within the Scheldt estuary, i.e. the brackish, deep area around the harbour of Antwerp (km 80) and the fresh water, shallow zone situated in the tidal estuary, about 40 km upstream from the former.

Longitudinal profiles of SPM and of k_d show a strong landwards decrease of the water transparency (Fig. 14). However, the complexity of the forcing functions and of their temporal interactions makes the direct interpretation of this pattern rather difficult. Indeed, when applying our reservoir model to both selected locations, a positive net phytoplankton growth is predicted at the more turbid one (location 1, Fig. 15a), whereas a negative net phytoplankton growth is simulated at location 2, in spite of the lower SPM concentration (Fig. 15b). In the absence of longitudinal transport, our model predicts a three-fold increase in algal biomass (expressed as chlorophyll *a* concentration) over a one-month period at location 1. In contrast, the chlorophyll *a* value is reduced by a factor of about 30% at location 2 within the same period. The main reason for this behaviour originates from the difference in z_{max} at both sites, location 2 displaying a mean water depth approximately twice as large as the value at location 1. These results are in agreement with the rapid drop in chlorophyll *a* concentration that is observed between the two locations (Fig. 16). They are consistent with the hypothesis that the euphotic to mixing depth ratio is the principal controlling factor of phytoplankton dynamics in this type of estuary. To evaluate the effect of a short-time photoacclimation on GPP and NPP, we considered a sinusoidal variation of α^B and P^B_{max}, both having a period of 24 h and an amplitude equal to 40% of the constant value in Table 1. We have tested the case of a peak for photosynthetic parameters in late morning-noon (see Prézelin, 1992), and inversely the case of a minimum in late morning-noon (see Harding et al., 1986). A diel-variation of α^B and P^B_{max} significantly affect phytoplankton growth during the month. When photosynthetic parameters exhibit a maximum value at noon, the model predicts a four-fold increase in algal biomass over a one-month period at location 2, and a slight decrease in chlorophyll *a* at location 1. On the other hand, if photosynthetic parameters exhibit a minimum value at noon, then chlorophyll *a* con-

centration increases by only 50% at location 2 over a month, and it decreases by 50% at location 1. Depending on the diel pattern taken into account, photoacclimation may thus enhance or reduce the phytoplankton production, but the overall conclusion remain unaffected. Interestingly, considering the possible effect of photoacclimation even reinforces the importance of using a time-dependent k_d instead of a constant mean value. It has already been shown (see 1st set of simulation) that the month-integrated GPPz computed with a time-dependent k_d was 30% higher than the value obtained using an average k_d. When considering a diel-variation of α^B and P^B_{max}, this difference between the month-integrated GPPz's increases from 30 to 67%, when photosynthetic parameters exhibit their minimum value at noon, and to 75% when they exhibit a peak at noon.

5 Conclusions

A number of hypothesis have been invoked to explain the well recognized phytoplankton decay that is often observed along the longitudinal salinity gradient of turbid, macrotidal estuaries. Among those, factors such as salinity stress, zooplankton grazing and light limitation due to the presence of a turbidity maximum, have been advocated (Soetaert et al., 1994; Kromkamp and Peene, 1995; Vanderborght et al., 2002). In this paper, we have shown that a net positive phytoplankton production can be sustained in areas of high turbidity, as long as the euphotic to mixing depth ratio remains sufficiently high. Conversely, deeper areas exhibiting lower turbidity might not be able to support a net biomass production, independently of any other biogeochemical influences. We have also demonstrated that the interplay between tidal and nychtemeral oscillations has to be resolved at least at the hourly timescale. This is a direct consequence of the different frequencies of the physical forcing functions (E_0, k_d, z_{max}), which results in a complex pattern of phytoplankton production at this timescale. Comparison between simulations using temporally resolved and averaged forcing functions indicate that the latter approach leads to significant errors in the estimation of estuarine productivity.

Acknowledgements. We wish to thank D. Bajura, M. Loijens and N. Roevros for their participation in analytical work and field missions. The support of the "Administratie Waterwegen en Zeewezen" of the Ministry of the Flemish Community and of the MUMM (Management Unit of the Mathematical Model of the North Sea, Royal Belgian Institute of Natural Sciences) is gratefully acknowledged. This research has been supported by the E.U. project EUROTROPH (EVK3-CT-2000-00040). The Belgian FRIA ("Fonds pour la Recherche dans l'Industrie et l'Agriculture") and the "Fondation Baron Van Buuren" have granted the work of one of the authors (X.D.).

References

Boyer, J. N., Christian, R. R., and Stanley, D. W.: Patterns of phytoplankton primary productivity in the Neuse River estuary, North Carolina, USA, Mar. Ecol. Prog. Ser., 97, 287–297, 1993.

Cloern, J. E.: Turbidity as a control on phytoplankton biomass and productivity in estuaries, Continental Shelf Research, 7, 1367–1381, 1987.

Cloern, J. E., Powell, T. M., and Huzzey, L. M.: Spatial and temporal variability in South San Francisco Bay (USA), II. Temporal changes in salinity, suspended sediments, and phytoplankton biomass and productivity over tidal time scales, Estuarine, Coastal and Shelf Science, 28, 599–613, 1989.

Cole, B. E.: Temporal and spatial patterns of phytoplankton production in Tomales Bay, California, USA, Estuarine, Coastal and Shelf Science, 28, 103–115, 1989.

Cole, B. E. and Cloern, J. E.: Significance of biomass and light availability to phytoplankton productivity in San Francisco Bay, Mar. Ecol. Prog. Ser., 17, 15–24, 1984.

Cole, B. E. and Cloern, J. E.: An empirical model for estimating phytoplankton productivity in estuaries, Mar. Ecol. Prog. Ser., 36, 299–305, 1987.

Cole, J. J., Caraco, N. F., and Peierls, B. L.: Can phytoplankton maintain a positive carbon balance in a turbid, freshwater, tidal estuary?, Limnology and Oceanography, 37, 1608–1617, 1992.

Cullen, J. J. and Lewis, M. R.: The kinetics of algal photoadaptation in the context of vertical mixing, Journal of Plankton Research, 10, 1039–1063, 1988.

de Jonge, V. N. and van den Bergs, J.: Experiments on the resuspension of estuarine sediments containing benthic diatoms, Estuarine, Coastal and Shelf Science, 24, 725–740, 1987.

Demers, S., Legendre, L., and Therriault, J.-C.: Phytoplankton responses to vertical tidal mixing, In: Tidal mixing and plankton dynamics, edited by Bowman, J., Yentsch, M., and Peterson, W. T., Springer-Verlag Berlin Heidelberg, 1986.

Demers, S., Therriault J.-C., Bourget, E., and Abdourrahmane, B.: Resuspension in the shallow sublittoral zone of a macrotidal estuarine environment: wind influence, Limnology and Oceanography, 32, 327–339, 1987.

Di Toro, D. M.: Optics of turbid estuarine waters: approximation and application, Wat. Res., 12, 1059–1068, 1978.

Falkowski, P. G. and Raven, J. A.: Aquatic Photosynthesis, Blackwell Science, Ltd., 1997.

Fasham, M. J. R.: Variations in the seasonal cycle of biological production in subarctic oceans: a model sensitivity analysis, Deep-Sea Research I, 42, 1111–1149, 1995.

Fettweis, M., Sas, M., and Monbaliu, J.: Seasonal, neap-spring and tidal variation of cohesive sediment concentration in the Scheldt estuary, Belgium, Estuarine, Coastal and Shelf Science, 47, 21–36, 1998.

Fichez, R., Jickells, T. D., and Edmunds, H. M.: Algal blooms in high turbidity, a result of the conflicting consequences of turbulence on nutrient cycling in a shallow water estuary, Estuarine, Coastal and Shelf Science, 35, 577–592, 1992.

Geider, R. J., MacIntyre, H. L., and Kana, T. M.: A dynamic model of photoadaptation in phytoplankton, Limnology and Oceanography, 41, 1–15, 1996.

Geider, R. J., MacIntyre, H. L., and Kana, T. M.: Dynamic model of phytoplankton growth and acclimation: responses of the balanced growth rate and the chlorophyll a:carbon ratio to light, nutrient-limitation and temperature, Mar. Ecol. Prog. Ser., 148, 187–200, 1997.

Geider, R. J., MacIntyre, H. L., and Kana, T. M.: A dynamic regulatory model of phytoplanktonic acclimation to light, nutrients, and temperature, Limnology and Oceanography, 43, 679–694, 1998.

Gilstad, M., Johnsen, G., and Sakshaug, E.: Photosynthetic parameters, pigment composition and respiration rates of the marine diatom Skeletonema Costatum grown in continuous light and a 12:12 h light-dark cycle, Journal of Plankton Research, 15, 939–951, 1993.

Grobbelaar, J. U.: Phytoplankton productivity in turbid waters, Journal of Plankton Research, 7, 653–663, 1985.

Han, B.-P.: A mechanistic model of algal photoinhibition induced by photodamage to photosystem-II, J. Theor. Biol., 214, 519–527, 2002.

Hansell, D. A. and Carlson, C. A.: Net community production of dissolved organic carbon,

Global Biogeochemical Cycles, 12, 443–453, 1998.
Harding, L. W. J., Meeson, B. W., and Fisher, T. R. J.: Phytoplankton production in two east coast estuaries: photosynthesis-light functions and patterns of carbon assimilation in Chesapeake and Delaware Bays, Estuarine, Coastal and Shelf Science, 23, 773–806, 1986.
Heip, C. H. R., Goosen, N., Herman, P. M. J., Kromkamp, J., Middelburg, J. J., and Soetaert, K.: Production and consumption of biological particles in temperate tidal estuaries, Oceanography and Marine Biology: an Annual Review, 33, 1–149, 1995.
Irigoien, X. and Castel, J.: Light limitation and distribution of chlorophyll pigments in a highly turbid estuary: the Gironde (SW France), Estuarine, Coastal and Shelf Science, 44, 507-517, 1997.
I. R. M.: Bulletin Mensuel des Observations Climatologiques de l'Institut Royal Météorologique de Belgique, Juillet 1999, partie II, edited by Malcorps, H., 1999.
Kana, T. M., Geider, R. J. and Critchley, C.: Regulation of photosynthetic pigments in microalgae by multiple environmental factors: a dynamic balance hypothesis, New Phytologist, 137, 629–638, 1997.
Keller, A. A.: Estimating phytoplankton productivity from light availability and biomass in the MERL mesocosms and Narragansett Bay, Mar. Ecol. Prog. Ser., 45, 159–168, 1988.
Kirk, J. T. O.: Light and photosynthesis in aquatic ecosystems, 2nd edn. Cambridge University Press, 1994.
Kromkamp, J. and Peene, J.: Possibility of net phytoplankton primary production in the turbid Schelde Estuary (SW Netherlands), Marine Ecology Progress Series, 121, 249–259, 1995.
Kromkamp, J., Peene, J., van Rijswijk, P., Sandee, A., and Goosen, N.: Nutrients, light and primary production by phytoplankton and microphytobenthos in the eutrophic, turbid Westerschelde estuary (The Netherlands), Hydrobiologia, 311, 9–19, 1995.
Lancelot, C., Hannon, E., Becquevort, S., Veth, C., and de Baar, H. J. W.: Modeling phytoplankton blooms and carbon export production in the Southern Ocean: dominant controls by light and iron in the Atlantic sector in Austral spring 1992, Deep-Sea Research I, 47, 1621–1662, 2000.
Lancelot, C., Mathot, S., and Owens, N. J. P.: Modelling protein synthesis, a step to an accurate estimate of net primary production: Phaeocystis pouchetii colonies in Belgian coastal waters, Marine Ecology Progress Series, 32, 193–202, 1986.
Lancelot, C., Veth, C., and Mathot, S.: Modelling ice-edge phytopankton bloom in the Scotia-Weddell sea sector of the Southern Ocean during spring 1988, Journal of Marine Systems,

2, 333–346, 1991.
Langdon, C.: On the causes of interspecific differences in the growth-irradiance relationship for phytoplankton. II, A general review. Journal of Plankton Research, 10, 1291–1312, 1988.
Langdon, C.: The significance of respiration in production measurements based on oxygen, ICES Mar. Sci. Symp., 197, 69–78, 1993.
Lewitus, A. J. and Kana, T. M.: Light respiration in six estuarine phytoplankton species: contrasts under photoautotrophic and mixotrophic growth conditions, Journal of Phycology, 31, 754–761, 1995.
Litaker, W., Duke, C. S., Kenney, B. E., and Ramus, J.: Short-term environmental variability and phytoplankton abundance in a shallow tidal estuary, II. Spring and fall, Mar. Ecol. Prog. Ser., 94, 141–154, 1993.
Lucas, C. H.: Observations of resuspended diatoms in the turbid tidal edge, Journal of Sea Research, 50, 301–308, 2003.
Macedo, M. F., Ferreira, F. G., and Duarte, P.: Dynamic behaviour of photosynthesis-irradiance curves determined from oxygen production during variable incubation periods, Mar. Ecol. Prog. Ser., 165, 31–43, 1998.
MacIntyre, H. L. and Cullen, J. J.: Primary production by suspended and benthic microalgae in a turbid estuary: time-scales of variability in San Antonio Bay, Texas, Mar. Ecol. Prog. Ser., 145, 245–268, 1996.
MacIntyre, H. L., Kana, T. M., Anning, T., and Geider, R. J.: Photoacclimation of photosynthesis irradiance response curves and photosynthetic pigments in microalgae and cyanobacteria (Review), Journal of Phycology, 38, 17–38, 2002.
Mague, T. H., Friberg, E., Hughes, D. J., and Morris, I.: Extracellular release of carbon by marine phytoplankton: a physiological approach, Limnology and Oceanography, 25, 262–279, 1980.
Malinsky-Rushansky, N. Z. and Legrand, C.: Excretion of dissolved organic carbon by phytoplankton of different sizes and subsequent bacterial uptake, Mar. Ecol. Prog. Ser., 132, 249–255, 1996.
Mallin, M. A. and Paerl, H. W.: Effects of variable irradiance on phytoplankton productivity in shallow estuaries, Limnology and Oceanography, 37, 54–62, 1992.
Melis, A.: Photosystem-II damage and repair cycle in chloroplasts: what modulates the rate of photodamage in vivo?, Trends in Plant Science, 4, 130–135, 1999.
Morán, X. A. G. and Estrada, M.: Phytoplanktonic DOC and POC production in the Bransfield

and Gerlache Straits as derived from kinetic experiments of ^{14}C incorporation, Deep-Sea Research II, 49, 769–786, 2002.
Muylaert, K., Van Nieuwerburgh, L., Sabbe, K., and Vyverman, W.: Microphytobenthos communities of the brackish to freshwater tidal reaches of the Schelde estuary (Belgium), Belgian Journal of Botany, 135, 15–26, 2002.
Otero, A. and Vincenzini, M.: Nostoc (cyanophyceae) goes nude: extracellular polysaccharides serve as a sink for reducing power under unbalanced C/N metabolism, Journal of Phycology, 40, 74–81, 2004.
Pahl-Wostl, C. and Imboden, D.M.: DYPHORA – a dynamic model for the rate of photosynthesis of algae, Journal of Plankton Research, 12, 1207–1221, 1990.
Platt, T., Gallegos, C. L., and Harrison, W. G.: Photoinhibition of photosynthesis in natural assemblages of marine phytoplankton, J. Mar. Res., 38, 687–701, 1980.
Postma, H.: Sediment transport and sedimentation, in: Chemistry and Biogeochemistry of Estuaries, edited by Olausson, E. and Cato, I., John Wiley and Sons Ltd., 153–186, 1980.
Prézelin, B.B.: Diel periodicity in phytoplankton productivity, Hydrobiologia, 238, 1–35, 1992.
Regnier, P., Mouchet, A., Wollast, R., and Ronday, F.: A discussion of methods for estimating residual fluxes in strong tidal estuaries, Continental Shelf Research, 18, 1543–1571, 1998.
Regnier, P. and Steefel, C. I.: A high resolution estimate of the inorganic nitrogen flux from the Scheldt estuary to the coastal North Sea during a nitrogen-limited algal bloom, spring 1995, Geochimica et Cosmochimica Acta, 63, 1359–1374, 1999.
Reid, P. C., Lancelot, C., Gieskes, W. W. C., Hagmeier, E., and Weichart, G.: Phytoplankton of The North Sea and its dynamics: a review, Netherlands Journal of Sea Research, 26, 295–331, 1990.
Soetaert, K., Herman, P. M. J., and Kromkamp, J.: Living in the twilight: estimating net phytoplankton growth in the Westerschelde estuary (The Netherlands) by means of an ecosystem model (MOSES), Journal of Plankton Research, 16, 1277–1301, 1994.
Steemann Nielsen, E. and Hansen, V. Kr.: Measurements with the carbon-14 technique of the respiration rates in natural populations of phytoplankton, Deep-Sea Research I, 5, 222–233, 1959.
Sverdrup, H. U.: On conditions for the vernal blooming of phytoplankton, J. Cons. Explor. Mer., 18, 287–295, 1953.
Vanderborght, J. P., Wollast, R., Loijens, M., and Regnier, P.: Application of a transport-reaction model to the estimation of biogas fluxes in the Scheldt estuary, Biogeochemistry, 59, 207–

237, 2002.
Verbanck, M.: Sediment-laden flows over fully-developed bedforms: first and second harmonics in a shallow, pseudo-2D turbulence environment, in: Shallow Flows, edited by Jirka, G. H. and Uijttewaal, W. S. J., Tu Delft, II 231–II 236, 2003.
Weger, H. G., Herzig, R., Falkowski, P. G., and Turpin, D. H.: Respiratory losses in the light in a marine diatom: measurements by short-term mass spectrometry, Limnology and Oceanography, 34, 1153–1161, 1989.
Williams, P. J. I. and Lefèvre, D.: Algal ^{14}C and total carbon metabolisms, 1. Models to account for the physiological processes of respiration and recycling, Journal of Plankton Research, 18, 1941–1959, 1996.
Wofsy, S. C.: A simple model to predict extinction coefficients and phytoplankton biomass in eutrophic waters, Limnology and Oceanography, 28, 1144–1155, 1983.
Wollast, R.: The Scheldt estuary, in: Pollution of the North Sea: an assessment, edited by Salomons, W., Bayne, B. L., Duursma, E. K., and Förstner, U., Springer-Verlag, 183–193, 1988.

Table 1. Notation, value and units of the parameters used in the model.

Parameters	Notation	Value	Units
Specific photosynthetic efficiency	α^B	0.05	(μgC.μgChl^{-1}.h^{-1}). (μmol quanta.m^{-2}.s^{-1})$^{-1}$
Specific light-saturation rate of photosynthesis	$P^B_{\max}$	13	μgC.μgChl^{-1}.h^{-1}
Rate constant for maintenance respiration	ρ_m	0.002	h^{-1}
Growth respiration factor	ρ_g	0.3	none
Excretion factor	ε	0.03	none
Rate constant for mortality	m	0.002	h^{-1}
Carbon: Chlorophyll α ratio	θ	50	gC.gChl^{-1}
Sediment transport coefficient (scenario 1)	X	2000	mg.L^{-1}.m^3.s^{-5}
Sediment transport coefficient (scenario 2)	X	6000	mg.L^{-1}.m^3.s^{-5}
Wash load (scenario 1)	Y	40	mg.L^{-1}
Wash load (scenario 1)	Y	25	mg.L^{-1}

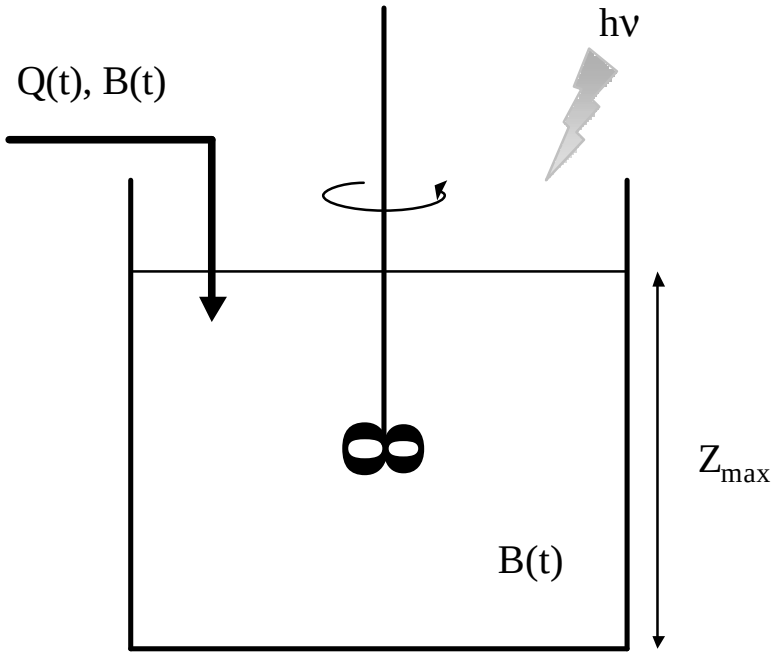

Fig. 1. Schematic representation of an oscillating-depth reservoir ($Q(t)$ = input/output flow; $B(t)$ = biomass concentration).

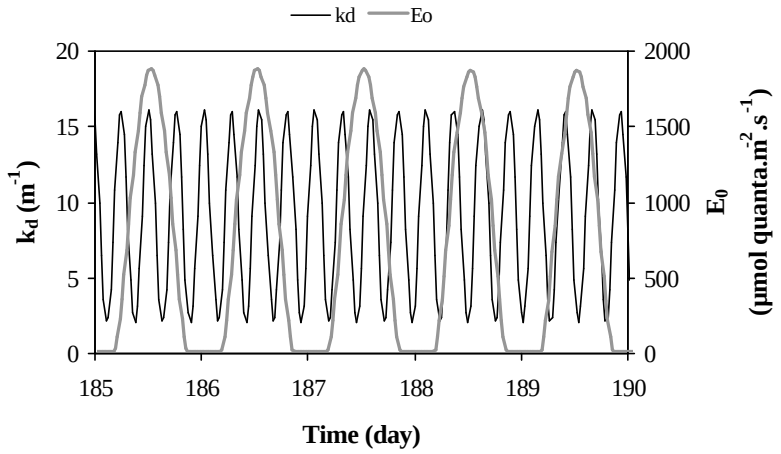

Fig. 2. Periodic forcing functions for the 1st set of simulations: light attenuation coefficient for scalar irradiance (k_d) and incident solar PAR (E_0).

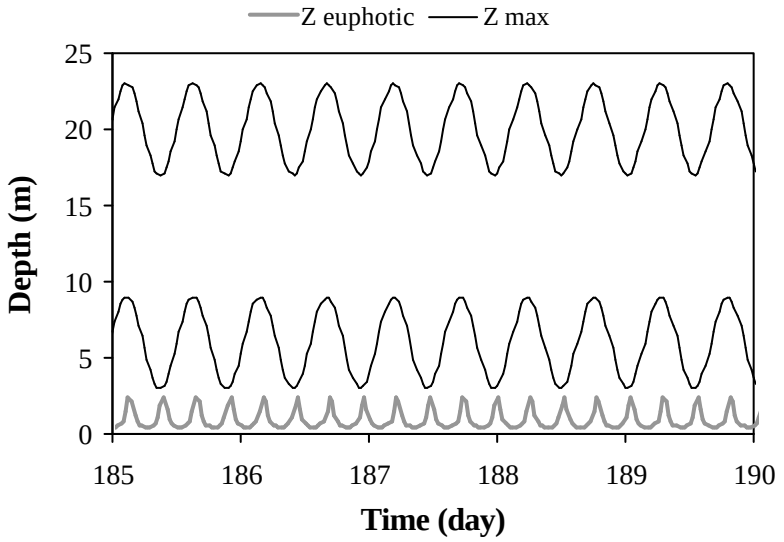

Fig. 3. Periodic forcing functions for the 1st set of simulations. Euphotic depth is taken as depth where 1% of incident light is reached. Mixing depths oscillate around value 6 m (shallow area) and 20 m (deeper area).

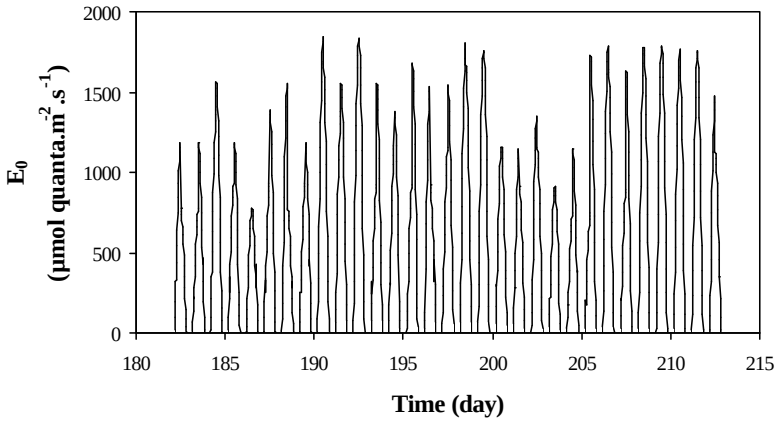

Fig. 4. Forcing functions for the 2nd set of simulations: incident solar PAR (July 1999, 52° N).

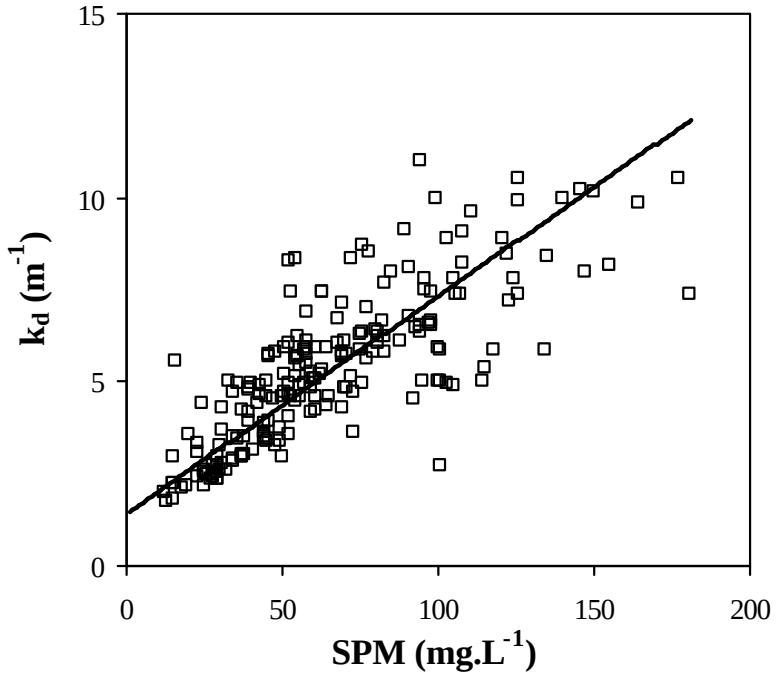

Fig. 5. Linear relationship between k_d and SPM as measured in the Scheldt estuary (k_d=1.4+0.0592×SPM; r^2=0.609).

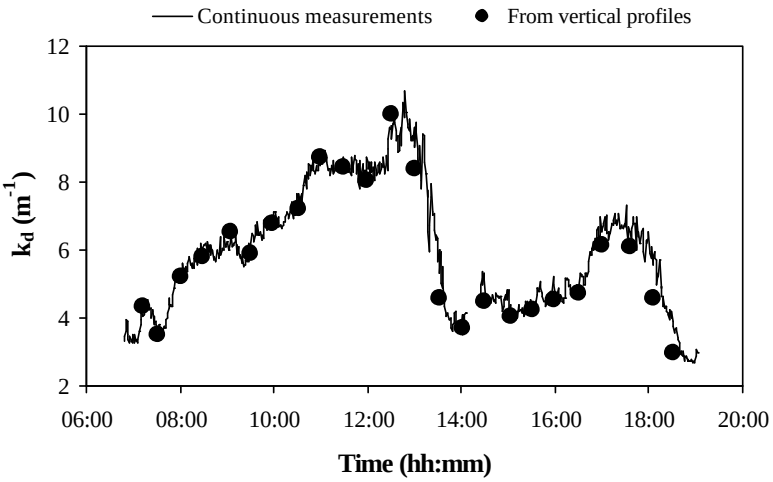

Fig. 6. Time variation of the light extinction coefficient for scalar irradiance during a complete tidal cycle (km 115, 22 August 2002).

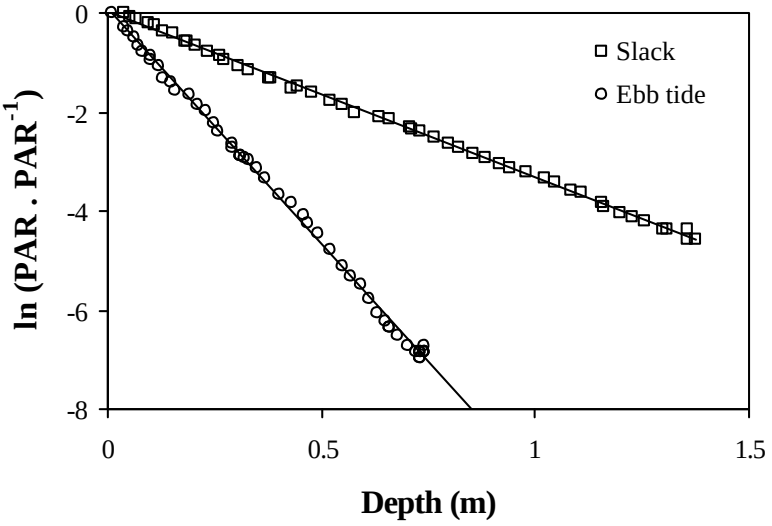

Fig. 7. Vertical profile of scalar irradiance measured in the tidal Scheldt estuary (km 115, 22 August 2002).

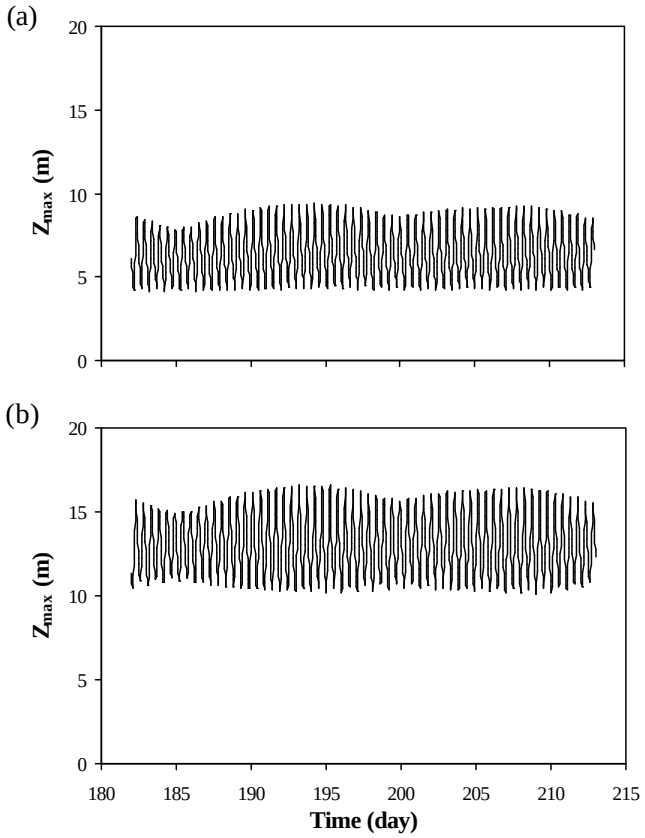

Fig. 8. Computed mixing depth for the 2nd set of simulations: **(a)** shallow area, **(b)** deeper area.

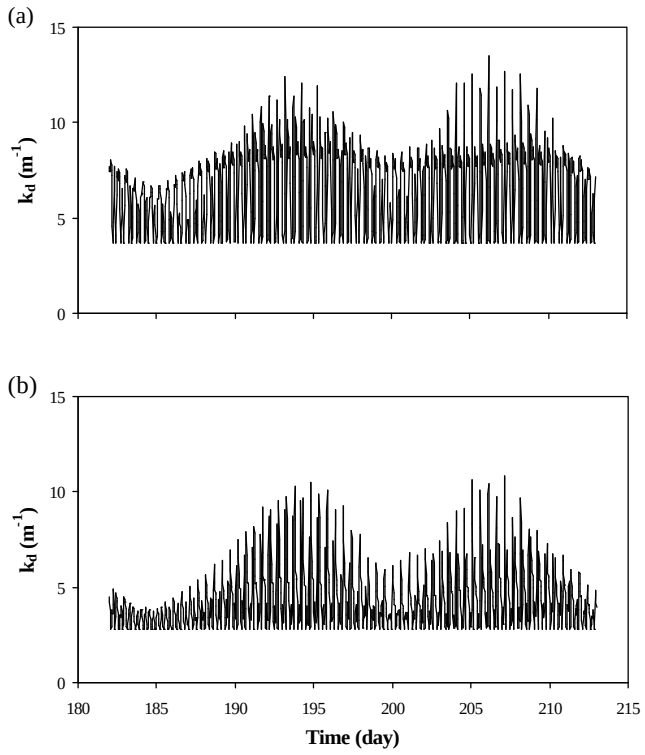

Fig. 9. Computed light attenuation coefficient for the 2nd set of simulations: **(a)** shallow area, **(b)** deeper area.

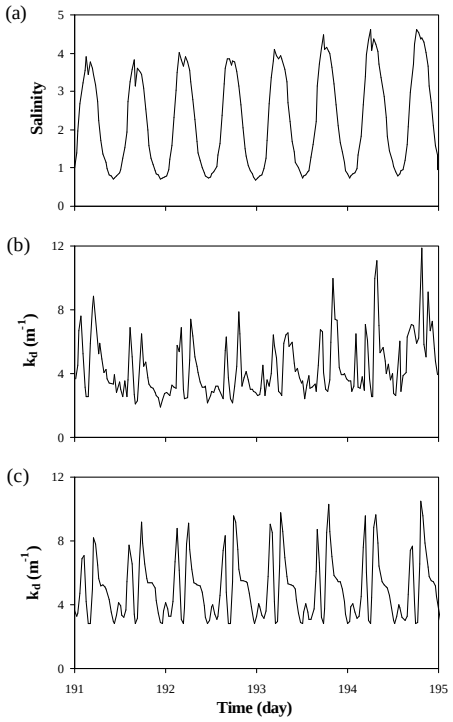

Fig. 10. Variation of **(a)** salinity and **(b)** the light attenuation coefficient as measured at a monitoring station in the Scheldt estuary (km 80, 10 to 14 July 1998). **(c)** Computed variation of the light attenuation coefficient (km 80, 10 to 14 July 1998).

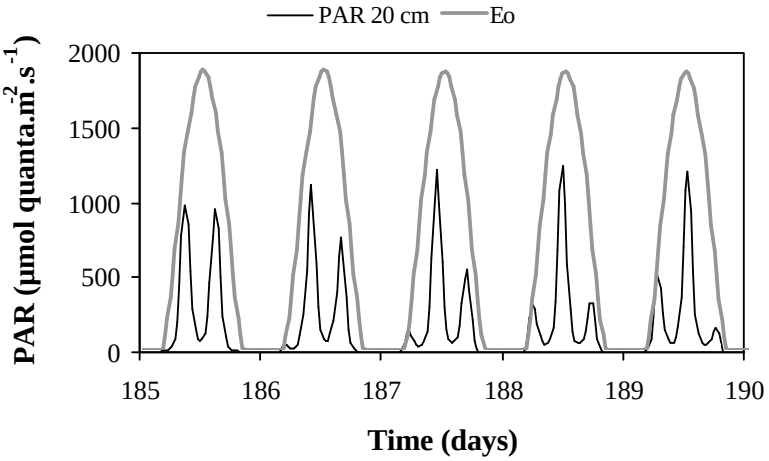

Fig. 11. Simulated incident solar light (PAR) at the surface of the water column and computed PAR at a 20 cm depth from 4 to 9 July.

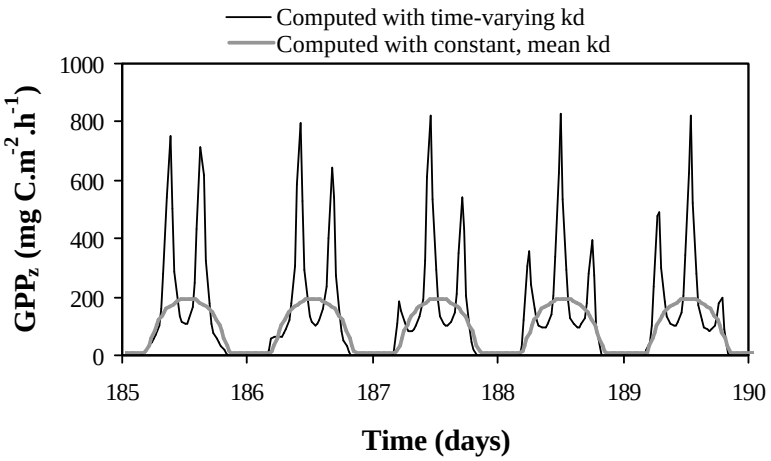

Fig. 12. Depth-integrated gross primary production (GPPz) from 4 to 9 July. GPPz computed using a time-varying k_d value and GPPz computed using a constant, mean k_d value.

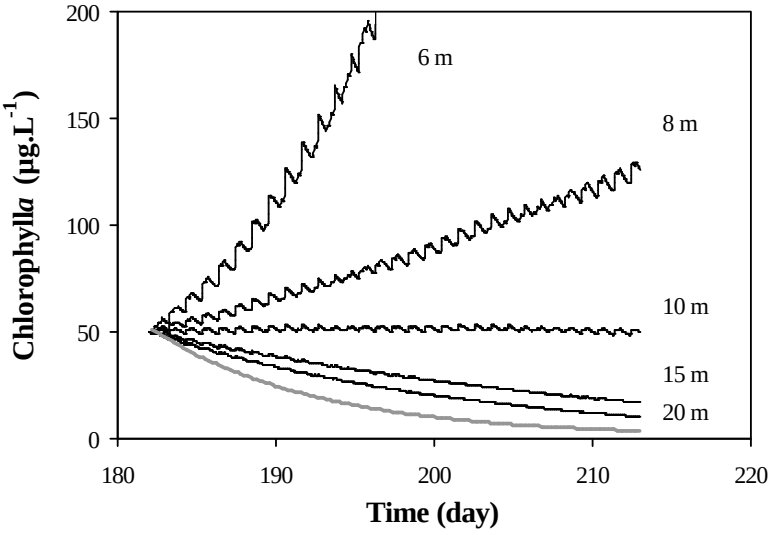

Fig. 13. Evolution of the net algal biomass (chlorophyll *a*) computed over a 30-days period. Mean z_{max} varies from 6 m to 20 m. Grey line corresponds to a situation with no production (exponential decrease).

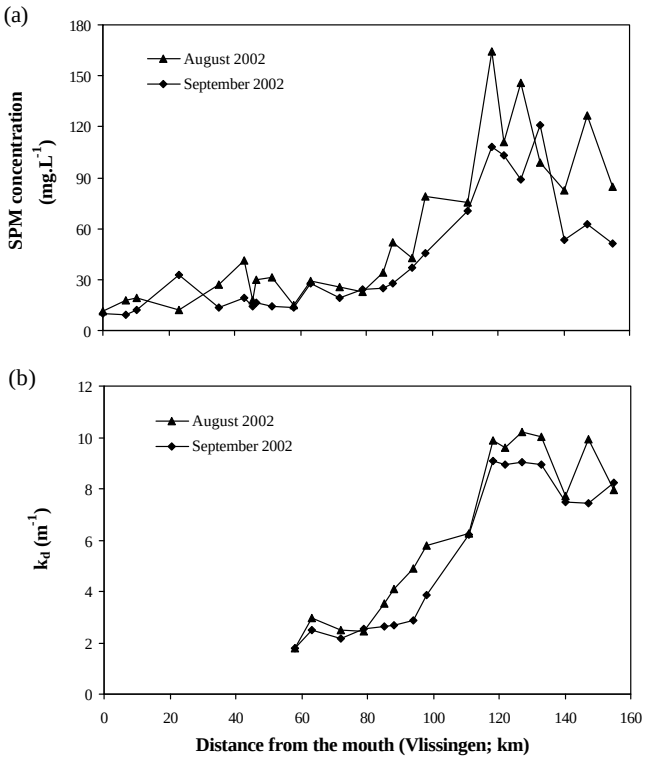

Fig. 14. Longitudinal distribution of **(a)** suspended solids concentration and **(b)** light attenuation coefficient along the Scheldt estuary. Location 1 (shallow area) is at km 120 and location 2 (deeper area) is at km 80.

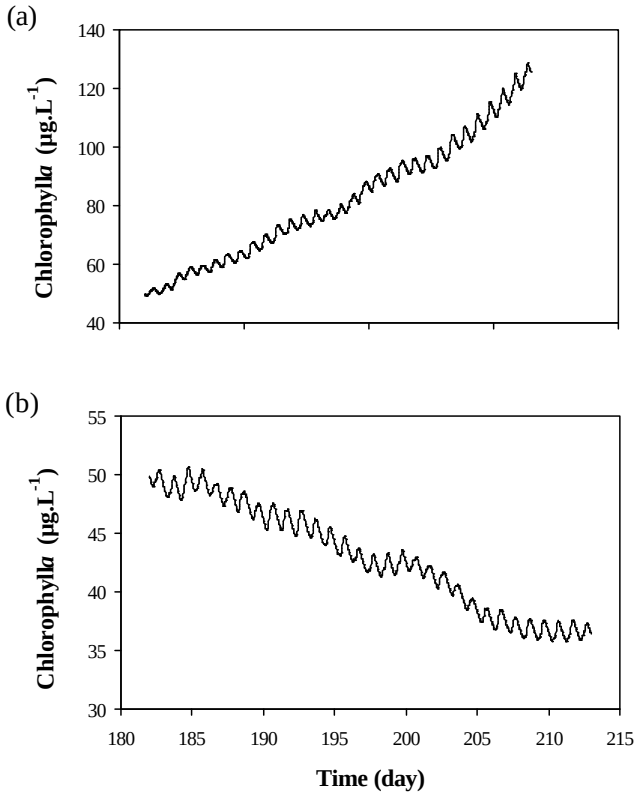

Fig. 15. Net chlorophyll *a* evolution during a 30-days simulation **(a)** for the shallow area and **(b)** for the deeper area.

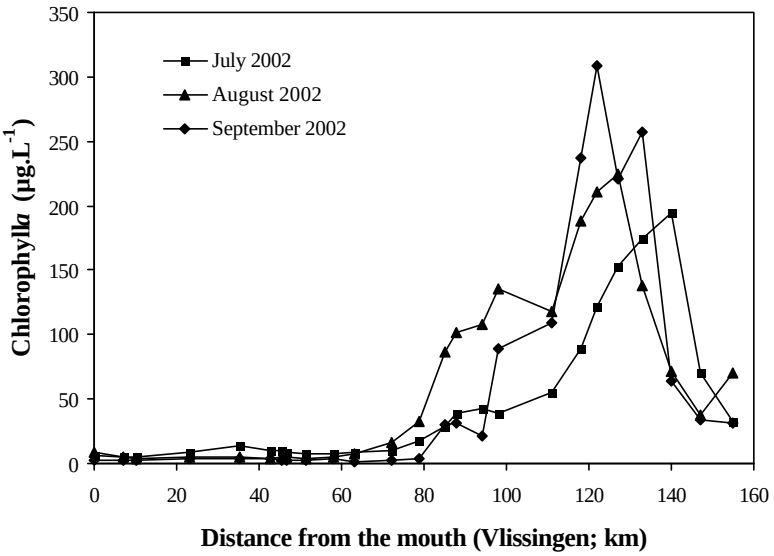

Fig. 16. Longitudinal profile of chlorophyll *a* concentration along the Scheldt estuary. Location 1 (shallow area) is at km 120 and location 2 (deeper area) is at km 80.